Electromagnetic Science
vol. 2, no. 2, 0060082, June 2024
https://doi.org/10.23919/emsci.2024.0008

Research Article

Frequency-Self-Adaptive Radio Frequency Power Harvester Enabled by Shape-Reconfigurable Liquid Metal

Cheng Zhang[1,2†], Yuchao Wang[1,2†], Zebin Zhu[1,2], Hai Lin[3], Kun Wang[3], Xintong Shi[3], Yi Du[4], Chaoyun Song[5,6], Long Ren[7], and Qiang Cheng[8]

1. *Key Laboratory of Materials for High-Power Laser*, *Shanghai Institute of Optics and Fine Mechanics*, *Chinese Academy of Sciences*, *Shanghai 201800*, *China*
2. *Hangzhou Institute for Advanced Study*, *University of Chinese Academy of Sciences*, *Hangzhou 310024*, *China*
3. *College of Physical Science and Technology*, *Central China Normal University*, *Wuhan 430000*, *China*
4. *Center of Quantum and Matter Science and School of Physics*, *Beihang University*, *Beijing 100191*, *China*
5. *Department of Engineering*, *King's College London*, *London WC2R 2LS*, *UK*
6. *State Key Laboratory of Radio Frequency Heterogeneous Integration*, *College of Electronics and Information Engineering*, *Shenzhen University*, *Shenzhen 518000*, *China*
7. *State Key Laboratory of Advanced Technology for Materials Synthesis and Processing*, *International School of Materials Science and Engineering*, *Wuhan University of Technology*, *Wuhan 430000*, *China*
8. *State Key Laboratory of Millimeter Waves*, *Southeast University*, *Nanjing 210096*, *China*

Corresponding authors: Chaoyun Song, Email: chaoyun.song@kcl.ac.uk; Long Ren, Email: renlong@whut.edu.cn; Qiang Cheng, Email: qiangcheng@seu.edu.cn.
†Cheng Zhang and Yuchao Wang contributed equally to this work.
Received February 23, 2024; Accepted June 5, 2024; Published Online June 18, 2024.

Abstract — Radio frequency (RF) energy harvester as an efficient tool for capturing and converting the flourishing ambient RF energy provides a promising solution for long-term powering the wireless sensor networks and the Internet of things (IoTs). However, the actual distribution of the environmental RF signals is dynamically frequency-dependent due to the diverse wireless terminals only interacting with specified frequencies. To take full advantage of the RF energy carrying this characteristic, an intelligent RF energy harvester is in demand to automatically sense the frequency information of an incident signal and conduct the corresponding RF-to-direct current transformation process. Here, to the best of my knowledge, a frequency-self-adaptive RF harvester is first presented with the help of the shape-reconfigurable liquid metal, which can precisely identify and efficiently convert an arbitrary signal from the frequency span of 1.8 to 2.6 GHz. Companied with a microcontroller unit and a tensile system, the dynamic functionality of the entire system is comprehensively demonstrated, showing promising potential to significantly advance various fields, including sustainable IoT applications, green wearable technologies, and self-powered devices.

Keywords — Liquid metal, Radio frequency power harvesting, Frequency-self-adaptive, Broadband rectification.
Citation — Cheng Zhang, Yuchao Wang, Zebin Zhu, *et al*., "Frequency-self-adaptive radio frequency power harvester enabled by shape-reconfigurable liquid metal," *Electromagnetic Science*, vol. 2, no. 2, article no. 0060082, 2024. doi: 10.23919/emsci.2024.0008.

I. Introduction

Amid the landscape of burgeoning wireless terminals and a looming energy crisis, radio frequency (RF) energy stands as a promising man-made renewable resource that has garnered substantial attention [1]–[3]. Unlike time-dependent renewable sources like solar [4]–[6] and tide [7], ambient RF power is perpetually accessible in densely populated areas [8]–[10], presenting a convenient avenue for harvesting and utilization. However, its inherent frequency characteristics, which have originally contributed to enhancing wireless communication speed and capability [11]–[12], paradoxi-

cally pose a challenge for RF energy harvesting. This challenge stems from the discrete signal channels of various technologies such as Bluetooth (2.4 GHz) [13], Wi-Fi (2.4 GHz and 5.8 GHz) [14], and the diverse bands of cellular networks like 5G (700 MHz, 1.9–2.6 GHz, 3.5 GHz, and 4.9 GHz) [15], each dynamically balanced and often regionally distributed [16]–[18]. In essence, while the continuous nature of ambient RF power is conducive to harvesting, the need to rectify this power into direct current (DC) introduces the requirement of recognizing the frequency information embedded in blind-source signals. Accomplishing this recognition and optimizing the capture performance of the harvester become a prerequisite. Thus, a compelling solution emerges: the imperative development of a novel frequency-self-adaptive RF energy harvester. This innovation would intelligently accommodate the ambient electromagnetic spectrum's variations and achieve efficient RF-to-DC conversion. Surprisingly, despite its significance, such research remains conspicuously absent thus far.

A classical RF energy harvester is traditionally comprised of two integral components: a receiving unit (typically an antenna [19]–[21] or metamaterial/metasurface [22]–[24]) responsible for capturing incoming RF signals, and a corresponding RF-to-DC conversion segment (usually a rectifier) [25]–[27]. Within this established design framework, achieving a frequency-self-adaptive RF energy harvester necessitates the incorporation of two intertwined elements: a frequency-reconfigurable receiver and a converter optimized to match the operational bandwidth. While extensive research has been conducted on broadband converters [28]–[30], the dynamic receiver component still faces certain limitations, including challenges related to modulation bandwidth and depth [31]–[33]. Consequently, a compelling avenue for scientific investigation lies in the advancement of receiver technologies. Recent developments have introduced the concept of employing p-type-intrinsic-n-type (PIN)-diode-embedded antennas, which offer the ability to discretely control their operational frequencies through the manipulation of integrated PIN diode states, toggling between the "ON" and "OFF" states to achieve this control [34]–[36]. For instance, a receiving antenna containing six PIN diodes was designed in [35], which can support 36 frequency states in a broad frequency range from 2.35 to 3.43 GHz. Nevertheless, the extent of tunable frequencies achievable through this approach remains constrained by the number of PIN diodes employed – specifically, utilizing n PIN diodes allows for a maximum realization of $2n$ coherent states, lacking the capacity for the requisite degree of arbitrary control. In response to these limitations, the integration of varactor diodes has been explored to establish tunable receiving antennas [37]. These antennas enable continuous adjustment of their operational frequency within a confined frequency range, achieved by smooth variations in the capacitance of the embedded varactor diodes. However, the potential of this method is inherently curtailed by the fixed receiver pattern and the constrained range of varactor diode modulation. Consequently, the dynamic modulation range for operational frequency remains challenging to significantly expand using this technique, limiting its practical applicability.

Interestingly, both aforementioned strategies rely on the manipulation of the antenna's equivalent capacitance, guided by classical LC resonance principles [37]. However, in order to make substantial strides in enhancing dynamic performance, it becomes imperative to introduce novel design paradigms that offer greater flexibility for constructing highly efficient RF power receivers. An important consideration is that the receiver's equivalent capacitance and inductance, which play a pivotal role in determining its operational frequency, are directly influenced by its pattern structure [38]. Thus, a breakthrough can be achieved by reconfiguring the pattern to suit specific requirements. In this regard, numerous efforts have been made to address these urgent needs, resulting in a plethora of new technologies such as origami [39], "magic angle" [40], and shape memory materials [41]. However, due to the limitations of complex 3D or 2D configurations and performance stability, these strategies still lack practical applications in electromagnetic-feature-reconfigurable antennas. In fact, to fulfill the above-mentioned needs, highly conductive materials with deformation properties are necessary, of which the electrical conductivity can maintain stable despite deformation. Based on these considerations, liquid metal (LM) boasts outstanding electrical conductivity and fluidity, making it an ideal candidate for achieving the desired functionalities [42], [43]. Nowadays, taking advantage of these unique merits, LM has been widely adopted to implement flexible pressure sensors [44], [45], temperature sensors [44], current limiter [46], and phase shifters [47]. Besides, lots of dynamic RF devices also have been achieved with the help of LM, such as frequency-reconfigurable antennas [48]–[57], radiation pattern-reconfigurable antennas [58], [59], bandwidth-reconfigurable antennas [60], and stretchable filter [61], reflecting the sufficient possibilities of using LM to realize the desired object.

Herein, leveraging the capabilities of LM, we introduce an innovative frequency-tunable RF energy harvester, as illustrated in Figures 1(a) and (c). The architecture encompasses an LM-based mechanically frequency-reconfigurable receiving antenna and a high-efficiency broadband rectifier network, facilitating exceptional RF-to-DC conversion efficiency across the spectrum from 1.8 to 2.6 GHz. Crucially, our design features a dual "∞"-shaped receiver deliberately engineered to ensure continuous frequency tuning within the band of 1.46 to 2.7 GHz. This tuning aligns seamlessly with the converter's frequency range, and it can be achieved by applying external strain up to 100%, following the interrelationship depicted in Figure 1(b). Expanding upon this foundation, we progress to the realization of a frequency-self-adaptive RF energy harvester, depicted in Figure 2(a). This advanced system integrates a microcontroller unit (MCU) and a comprehensive tensile system, en-

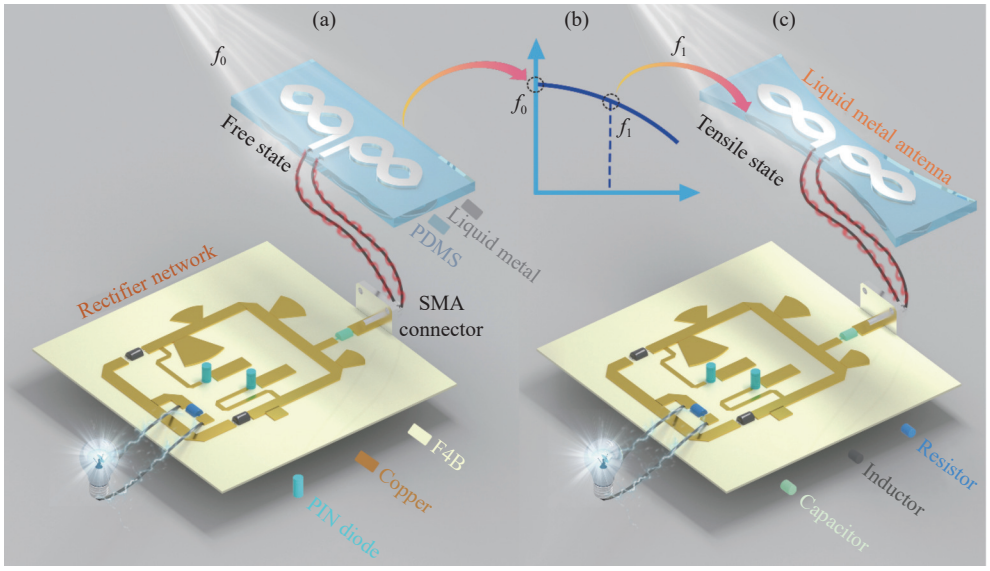

Figure 1 (a) Free state of the mechanically frequency-tunable RF energy harvester; (b) Relationship between operational frequency and tensile ratio of the LM-based antenna; (c) Tensile state of the frequency-tunable RF energy harvester. (F4B denotes the type of the dielectric plate; f_0 means the initial frequency; f_1 indicates another frequency diffenent from f_0; PDMS: polydimethylsiloxane).

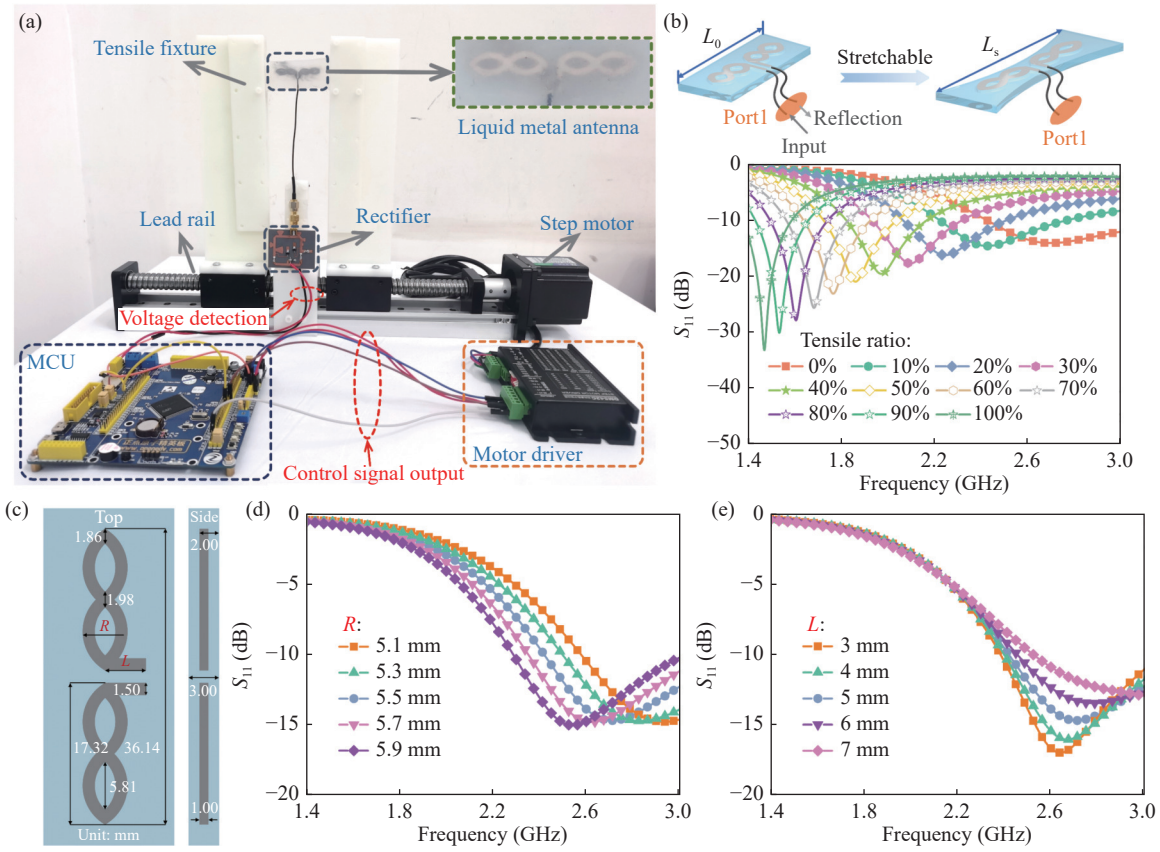

Figure 2 (a) Illustration of the proposed frequency-self-adaptive RF energy harvester. (b) Simulated port reflection coefficient S_{11} curves of the stretchable LM-based antenna under a tensile ratio varying from 0% to 100%. (c) Detailed structural parameters of the LM-based frequency reconfigurable antenna; Simulated S_{11} of the proposed antenna as a function of frequency with different values of (d) R and (e) L.

compassing a tensile fixture, lead rail, step motor, and its driver. The MCU, equipped with voltage detection capabilities, monitors the evolving DC voltage output from the rectifier network. Concurrently, it generates displacement signals to govern the step motor, orchestrating adjustments in strain applied to the LM-based antenna. Employing an intricately devised detection and feedback circuit, the LM-enhanced system adeptly discerns the frequency characteristics of the input signal. Subsequently, it fine-tunes the applied strain on the flexible antenna to align with an optimal

value based on their correlated relationship, akin to the depiction in Figure 1(b). This perpetual real-time adaptation ensures the maintenance of peak RF power reception, consequently yielding a corresponding optimal DC power output. In summary, through ingenious integration of LM technology, our research yields a frequency-tunable RF energy harvester, progressing into a self-adaptive configuration. This transformative technology boasts potential implications in the realm of energy harvesting, perpetuating optimal power capture through continuous frequency tracking and dynamic strain modulation.

II. Theory and Design

Before assembling the total system, an LM-based antenna for dynamically capturing the frequency-varying RF signal via changing the externally applied strain should be obtained first to determine the working frequency bandwidth. To achieve the frequency-reconfigurable functionality, as shown in Figure 2(b), a dual "∞"-shaped antenna is designed based on the LM and embedded into a flexible polydimethylsiloxane (PDMS) substrate with the relative permittivity of 4.2. Our design resembles a spring structure that can maintain shape stability when stretched even at great tensile ratios, favoring consistent radiation patterns.

We subjected the designed antenna configuration to a broadband RF signal spanning from 1.4 to 3.0 GHz, which was introduced through Port1 for unveiling its RF energy capture capabilities, as illustrated in Figure 2(b). Notably, with an incremental increase in the tensile ratio, a discernible trend emerges: the peak of the port reflection coefficient (S_{11}) progressively shifts towards lower frequencies (Figure 2(b)). This shift mirrors a coherent and monotonous relationship (shown by the orange solid line in Figure 3(a)), aligning harmoniously with the previously established requirement. Simultaneously, the corresponding RF energy capture capability is vividly depicted by the solid green line in Figure 3(a). Employing the reciprocity theorem [62], we deduce that the power ratio reflected and detected at Port1 (Figure 3(a)) provides a direct window into the receiving performance of our proposed antenna. Remarkably, even amid deformation, our design continues to exhibit robust RF energy capture prowess, attributed to the pronounced ultra-low reflection phenomenon at Port1. This alignment with the prerequisites for efficient energy harvesting showcases the design's adeptness. Furthermore, the actual characteristics of the fabricated sample (depicted in Figure 2(a)) were meticulously measured to validate their impact on the ultimate integrated system's performance. As depicted in Figure 3(a), the measured outcomes (indicated by star icons) closely reflect the simulated results, attesting to a high degree of consistency. Any disparities between the simulated and measured operational frequencies can be ascribed to the precision of RF cable positioning concerning the LM-based antenna pattern. The detailed procedure for the fabrication of the LM-based antenna and its tensile property are described in Supplementary Note S1 and Figure S1 of the **Supporting Information**. Note that the strong agreement endows the proposed antenna with working frequency selectivity as appropriate strain is applied, which can be regarded as the foundation of the final RF energy harvester. Here, it needs to be emphasized that when design this antenna, the effect of the curvature radius (R) of the "∞"-shaped structure (Figure 2(d)) and the length (L) of the feeding line (Figure 2(e)) on the S_{11} of the proposed LM-based antenna (Figure 2(c)) has been comprehensively analyzed to determine its structural parameters. As shown in Figure 2(d), with the increase of R, the corresponding resonance frequency of the antenna gradually moves to lower frequencies, which can be attributed to the growth of its electrical length. Therefore, to ensure the initial resonance frequency stay at 2.69 GHz (namely 5G band), 5.5 mm was selected as the optimal value of R. Additionally, the S_{11} of the antenna can be improved when the feeding line is shortened as shown in Figure 2(e). Finally, comprehensively considering the concomitant redshift, 5 mm was chosen as the value of L. The other detailed structural parameters of the reconfigurable antenna can be obtained in Figure 2(c).

Alongside its tunable working frequency and impressive RF power reception efficiency, another noteworthy aspect emerges when observing the surface currents along the dual "∞"-shaped patterns, as exemplified in Figure 3(b). These surface current distributions consistently exhibit the characteristic traits of a half-wavelength dipole, featuring maximal current densities at the center while gradually diminishing to zero along the antenna's arms [63]. This behavior resembles a sine function with half period, a pattern that endures even when considering variations in stretching ratios. This unique surface current pattern aligns harmoniously with classical electromagnetic theory, giving rise to the potential for omnidirectional radiation patterns. The inherent nature of the current distribution underscores the capability of our LM-based antenna to facilitate omnidirectional reception, even in the face of diverse incident angles. In essence, this further accentuates the advantageous position of our antenna design, proficiently capturing input RF power from a variety of angles. Subsequently, to verify the excellent radiation performance of the antenna under original and stretched states, the corresponding simulated three-dimensional (3D) (first row), simulated and measured two-dimensional (2D) (second row) radiation patterns are supplied in Figure 3(c). It is obvious the H-plane scattering pattern is evenly distributed in all directions while a "∞"-shaped pattern is in the orthogonal plane (namely E-plane), which is consistent with the radiation behaviors of a half-wavelength dipole antenna as predicted. Furthermore, the measured results consistently align with the simulated ones, even when the sample is subjected to different external strains, verifying the correctness of our design.

Then to further showcase the impact of stretching on the antenna performance, the realized gain, radiation efficiency and polarization feature of the stretchable LM-based

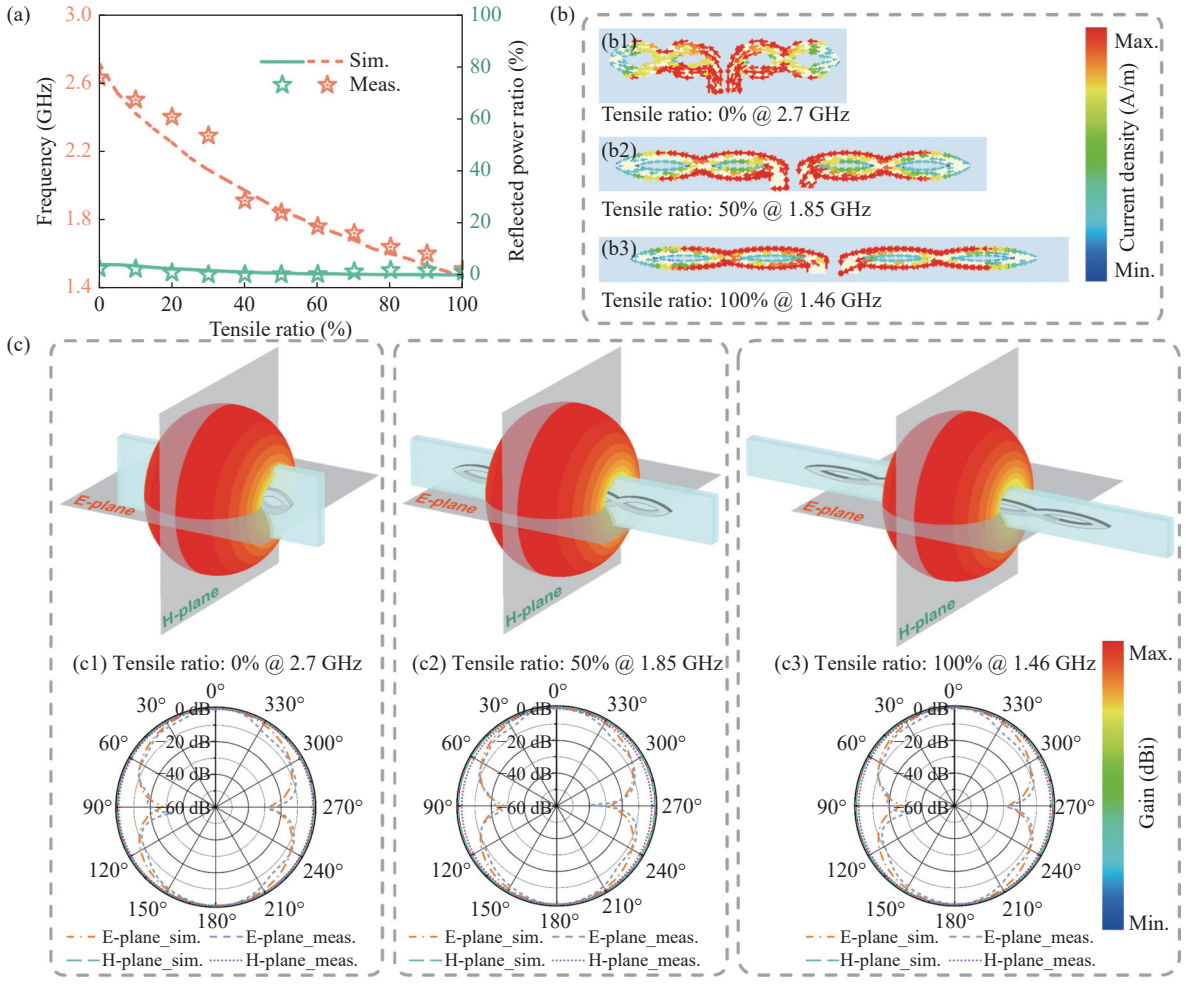

Figure 3 (a) Simulated and measured operation frequency and corresponding reflected power ratio of the stretchable antenna as a function of tensile ratio. (b) Surface currents and (c) 3D/2D radiation patterns of the stretchable antenna applied with different strains (corresponding different operation frequencies): (b1) and (c1) Free state @ 2.7 GHz; (b2) and (c2) Tensile ratio of 50% @ 1.85 GHz; (b3) and (c3) Tensile ratio of 100% @ 1.46 GHz. (Max. stands for maximum, Min. for minimum, sim. for simulation, meas. for measurement).

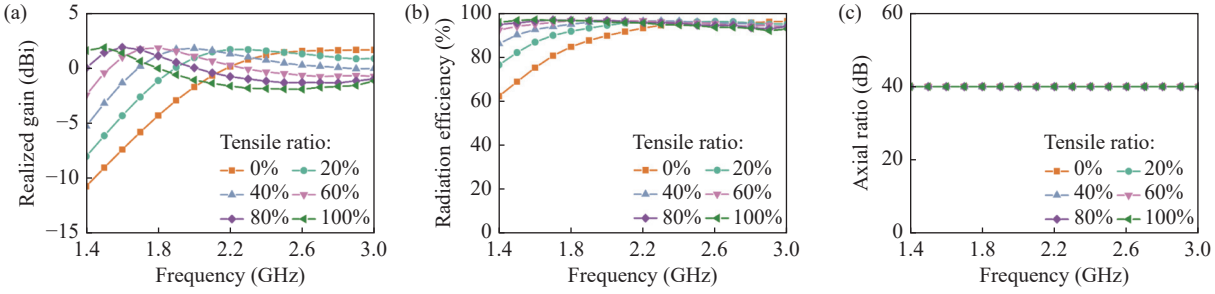

Figure 4 (a) Simulated realized gain, (b) radiation efficiency, and (c) axial ratio of the stretchable LM-based antenna as the tensile ratio varies from 0% to 100%.

antenna were simulated and presented in Figure 4. As shown in Figure 4(a), with the increase of the tensile ratio, the maximum realized gain of our design gradually shifts toward lower frequencies, conforming to the change regular of the resonance frequencies (shown in Figure 2(b) and Figure 3(a)). Additionally, the corresponding radiation efficiency at these frequencies can be significantly improved as the tensile ratio increases (Figure 4(b)), favoring the efficient capture of ambient RF power. Finally, the ultra-high axial ratio (about 40 dB, Figure 4(c)) proves that the polarization state of our design is independent of tensile degree. Considering the transmit-receive reciprocity property, our design is no doubt a promising choice for harvesting the ambient RF energy. In addition, the resonance frequency and the corresponding amplitude (shown in Figure 5) of the fabricated antenna are always stable after 1000 tensile cycles, proving the excellent durability and strong stability.

Analyzing the existing LM-based frequency reconfig-

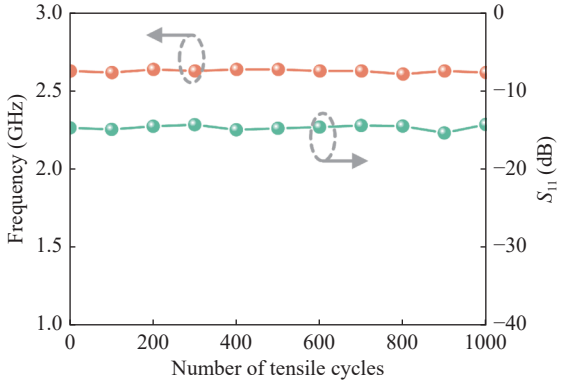

Figure 5 Working frequency and the corresponding S_{11} of the LM-based antenna after 100, 200, 300, 400, 500, 600, 700, 800, 900, and 1000 cycles of stretching (the applied strain repeatedly varies from 0% to ~100%).

urable antennas shown in Table 1 reveals that it is highly challenging to design an LM-based antenna with a large relative bandwidth where the radiation patterns remain stable during mechanical deformations. In contrast, thanks to the innovative design, our proposed antenna, to the best of our knowledge, exhibits maximum relative bandwidth (73%) while maintaining frequency continuity and stability of the radiation patterns as the operation frequency is tuned, making our design versatile for various application scenarios, including integration with other devices.

At this juncture, the realization of a frequency-tunable ambient RF power receiver has been successfully accomplished through the dynamic application of strain. The next pivotal step involves the integration of a broadband RF-DC converter, denoted as the rectifier network in Figure 6(a), designed to efficiently transform received RF power into DC energy. The converter's operational bandwidth is strategically selected to comprehensively encompass the tunable frequency range of the receiver. Given the typically modest power levels of ambient RF signals, the rectifier network must exhibit both exceptional RF-DC conversion efficiency at these power levels and a notable power handling capacity. To meet these dual criteria, we have developed an innovative rectifier network at the input power level of −10 dBm, as illustrated in Figure 6(a). This network encompasses a range of essential components, including a two-branch impedance matching circuit (highlighted in green) for transferring the input impedance of the rectifying network to the standard 50 Ω, a rectifying network (colored orange), a pair of PIN diodes (the detailed information of the adopted diode is provided in Figure 7) for RF-DC conversion, a DC-pass filter to enhance output smoothness, and a load resistor. The detailed structural parameters of the rectifier network can be found in Figure 6(c).

In pursuit of an enhanced operational bandwidth, our design adopts a two-branch structure, delineated as Branch1 and Branch2 within Figure 6(a). Branch1 caters to the frequency range of 1.8 to 2.0 GHz, while Branch2 corresponds to the span of 2.2 to 2.6 GHz (as shown in Figure 6(a)). Examining Figure 6(d), we consider the case of a broadband RF signal spanning from 1.5 to 3.0 GHz, carrying a power of 100 μW, directed into the rectifier network. Notably, power probe 1 (P_1), positioned ahead of the first PIN diode (D_1), effectively captures the majority of input power within the range of 1.8 to 2.0 GHz. Conversely, the power attributed to the range of 2.2 to 2.6 GHz predominantly flows through Branch2, leading to rectification by the second PIN diode (D_2). Significantly, both Branch1 and Branch2 collaboratively facilitate RF-DC conversion within the intermediate frequency band spanning 2.0 to 2.2 GHz, thereby endowing our design with a remarkable bandwidth spanning from 1.8 to 2.6 GHz. Beyond the expanded operational bandwidth, the corresponding RF-DC conversion efficiency, another pivotal metric, is unveiled in Figure 6(b). This parameter can be derived through the following equation:

$$\text{Efficiency} = V_{\text{out}}^2/(R_{\text{load}} \times P_{\text{in}}) \quad (1)$$

where R_{load} is the optimal load resistance of the rectifier

Table 1 Comparison of our LM-based antenna with other related works

Ref.	Frequency range (GHz)	Relative bandwidth	Frequency continuity	Radiation pattern stability	Maximum tensile ratio	Methodology
[48]	1.7–3.5	69%	Yes	NR	NA	Injection
[49]	1.8–3.1 3.2–5.4	53% 51%	No	No	NA	Injection
[50]	2.4 and 3.87	NA	No	Yes	NA	Injection
[51]	5.8–6.4	10%	No	No	NA	Injection
[52]	0.6–13.5	183%	Yes	No	NA	Injection
[53]	1.9–2.35 3.2–3.5	21% 9%	Yes	Yes	NA	Injection
[54]	2.78–2.93	5%	Yes	Yes	15%	Stretching
[55]	2.42–3.45	35%	Yes	NR	60%	Stretching
[56]	0.738–1.53	70%	Yes	NR	120%	Stretching
[57]	1.37–1.7	21%	Yes	Yes	30%	Stretching
This work	1.4–3.0	73%	Yes	Yes	100%	Stretching

Note: NR, not reported; NA, not acquired.

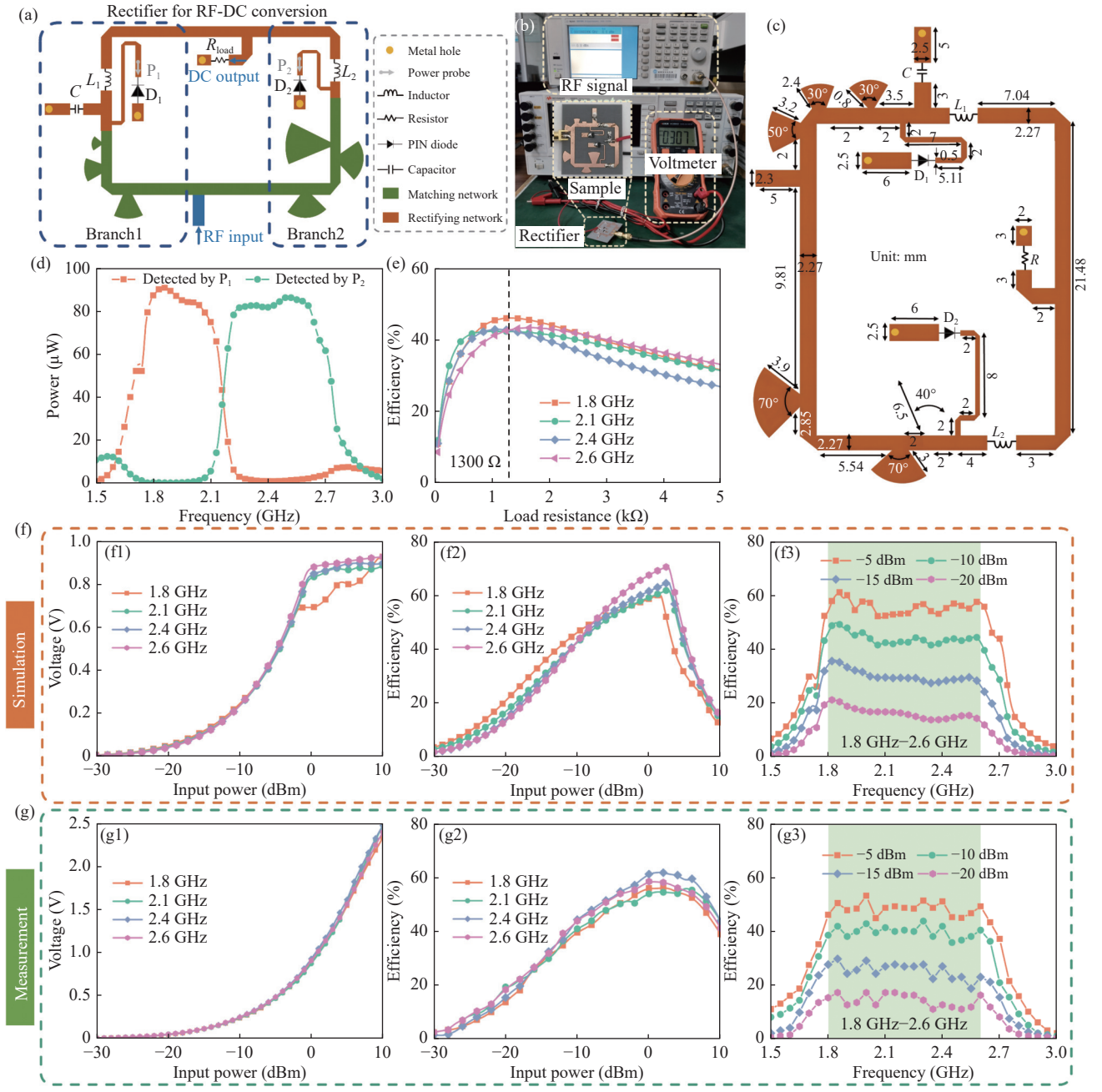

Figure 6 (a) Topology of the proposed broadband rectifier network for transforming the captured RF power (L_1, L_2: 22 nH; C: 10 pF); (b) Photograph of the RF-DC conversion efficiency measurement setup. (c) Detailed structural parameters of the rectifier network. (d) Detected power distribution by two power probes (P_1 and P_2) as the input power is set to 100 μW. (e) Simulated RF-DC conversion efficiency of the rectifier network as a function of load resistance at different frequencies. (f) and (g) Simulated and measured RF-DC conversion performance of the proposed rectifier network: (f1) and (g1) Output voltage vs. input power; (f2) and (g2) RF-DC conversion efficiency vs. input power; (f3) and (g3) RF-DC conversion efficiency vs. frequency.

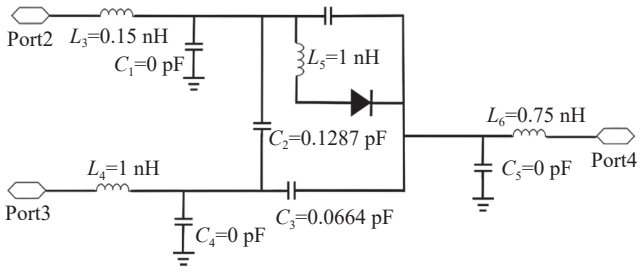

Figure 7 Equivalent circuit model and package parameters of the Schottky diode (SMS7630).

(1300 Ω which can support the optimal RF-DC conversion efficiency in the working bandwidth as shown in Figure 6(e)), P_{in} is the input power to the rectifier network illustrated in Figure 6(a), and V_{out} is the output voltage across the load resistance. By substituting the simulated input-power-dependent voltage output at different frequencies (Figure 6(f1)) into (1), then the theoretical efficiency can be calculated and presented in Figure 6(f2). Due to the linear characteristic of the PIN diode, the output voltage and conversion efficiency increase as the input power gradually en-

hances. However, once the PIN diodes are penetrated, the output voltage experiences saturation and stabilizes (as seen in Figure 6(f1)), while a diminishing efficiency becomes evident in Figure 6(f2) due to the heightened input power. Furthermore, the broadband nature of our design's capabilities is demonstrated in Figure 6(f3). When the input power is maintained at −10 dBm (equivalent to 100 μW), the simulated RF-DC conversion efficiency spans the working bandwidth, surpassing the 40% threshold. This efficacy ensures the optimal utilization of the RF power captured at the frontend. It is noteworthy that the nonlinear phenomena previously demonstrated in Figures 6(f2) are also evident in Figure 6(f3) as input power variations are considered. Subsequently, to validate the rectification performance of our proposed rectifier network, the rectifier was built on a Duroid 5880 substrate with the relative permittivity of 2.2, and a comprehensive measurement was conducted using the setup delineated in Figure 6(b). In this experimental arrangement, a signal generator (Agilent N9310A) and a voltmeter were employed to generate the required RF signal and measure the resulting DC voltage output, respectively. Comparing the measured DC voltage (Figure 6(g1)) to the simulated results in Figure 6(f1), a congruent trend is observed in relation to input power variations. Notably, the saturation of voltage is not as evident in the measured data due to the nonlinear current-voltage characteristics of the rectifying diode. Consequently, this leads to a slightly more gradual decline in measured efficiency, as illustrated in Figure 6(g2), compared to Figure 6(f2). Meanwhile, the broadband RF-DC conversion efficiency of the fabricated rectifier network (Figure 6(g3)) closely aligns with the simulated outcome presented in Figure 6(f3). Any minor deviations can be attributed to manufacturing precision and potential testing errors.

Ultimately, the core component of the mechanically frequency-self-adaptive RF energy harvester illustrated in Figure 2(a) can be built by jointing the LM-based RF power receiver (Figure 2(b)) with the performance-matched RF-DC converter (Figure 6(a)), and the total system (Figure 2(a)) will be evaluated in the following part.

III. System Performance Evaluation

Before delving into the dynamic performance measurement of the frequency-self-adaptive total system, a comprehensive understanding of the MCU's control logic is paramount. The MCU is equipped with the capability to detect the generated voltage and manage the step motor's actions in tuning the strain applied to the LM-based antenna. When presented with a specified frequency signal, the RF receiver undergoes continuous stretching, transitioning from its original state to a state with a tensile ratio of 100%. This extension is accomplished through the involvement of the step motor, where each step length is defined as 1 mm. Concurrently, utilizing the temporal intervals between successive steps, the MCU persistently gauges the dynamic voltage values and records corresponding tensile lengths. Following the completion of this intricate process, the maximum voltage can be readily identified through a comparison of the detected outcomes. Moreover, the optimal deformation ratio of the flexible antenna can be discerned. Subsequently, the MCU expeditiously configures the antenna to the determined tensile state through manipulating the step motor. Notably, the frequency-selective nature of the receiver bestows a unique feature: when the input signal is transformed to a frequency divergent from its initial state, the detected voltage experiences a notable decay, as anticipated by the trend in Figure 3(a). Consequently, this prompts the initiation of the previously described process, serving the purpose of sensing the newly set frequency and optimizing the DC output. Ultimately, by amalgamating the elaborately designed control circuit into the aforementioned control logic, the total system depicted in Figure 2(a) undergoes measurement within a microwave anechoic chamber (as illustrated in Figure 8(a)). In this setup, a horn antenna, linked to an RF signal generator, functioned as the transmitting source responsible for supplying the LM receiver.

Throughout the testing procedure, the receiving power of the total system was standardized at −10 dBm, attained by finely adjusting the output power of the signal generator. Subsequently, by systematically varying the frequency information of the input RF signal within the range of 1.5 to 2.6 GHz, automatic measurement of the tensile ratio and antenna length transpires. These measurements exhibit a linear correlation with the incident frequency (as exemplified in Figure 8(b)), consistently mirroring the simulated trends detailed in Figure 3(a). In addition, three demos for 2.6, 2.2, and 1.8 GHz have been provided in Figures 8(c)–(e), and their dynamic frequency adaptation process can be found in Supplementary Video S1 of the **Supporting Imformation** for showcasing the powerful capability of the novel system. Subsequently, in Figures 8(f)–(g), we present the simultaneously generated DC voltage from the total system alongside the corresponding achieved RF-DC efficiency. Evidently, the measured outcomes exhibit a strong alignment with the simulated results across an expansive frequency range. This span encompasses the Wi-Fi/WLAN band (2.4 GHz), traditional communication bands (1.8, 2.1, and 2.3 GHz), as well as the 5G band (2.6 GHz), effectively showcasing the excellent practical viability of our design.

It is worth noting that the primary aim of our work is to demonstrate the feasibility of using such a mechanically shifted adaptive system to sense and capture RF energy. Although the current system requires high power to drive all sub-system elements, including the motor and MCU, when the input energy is low, alternative low-power MCUs and motors could be employed to reduce the overall power consumption. To aid readers in understanding the roles and limitations of the MCU and motor, we have searched and compared several state-of-the-art components with those selected for this study, as detailed in Table S1 and Table S2 of the **Supporting Information**. Our findings show that by

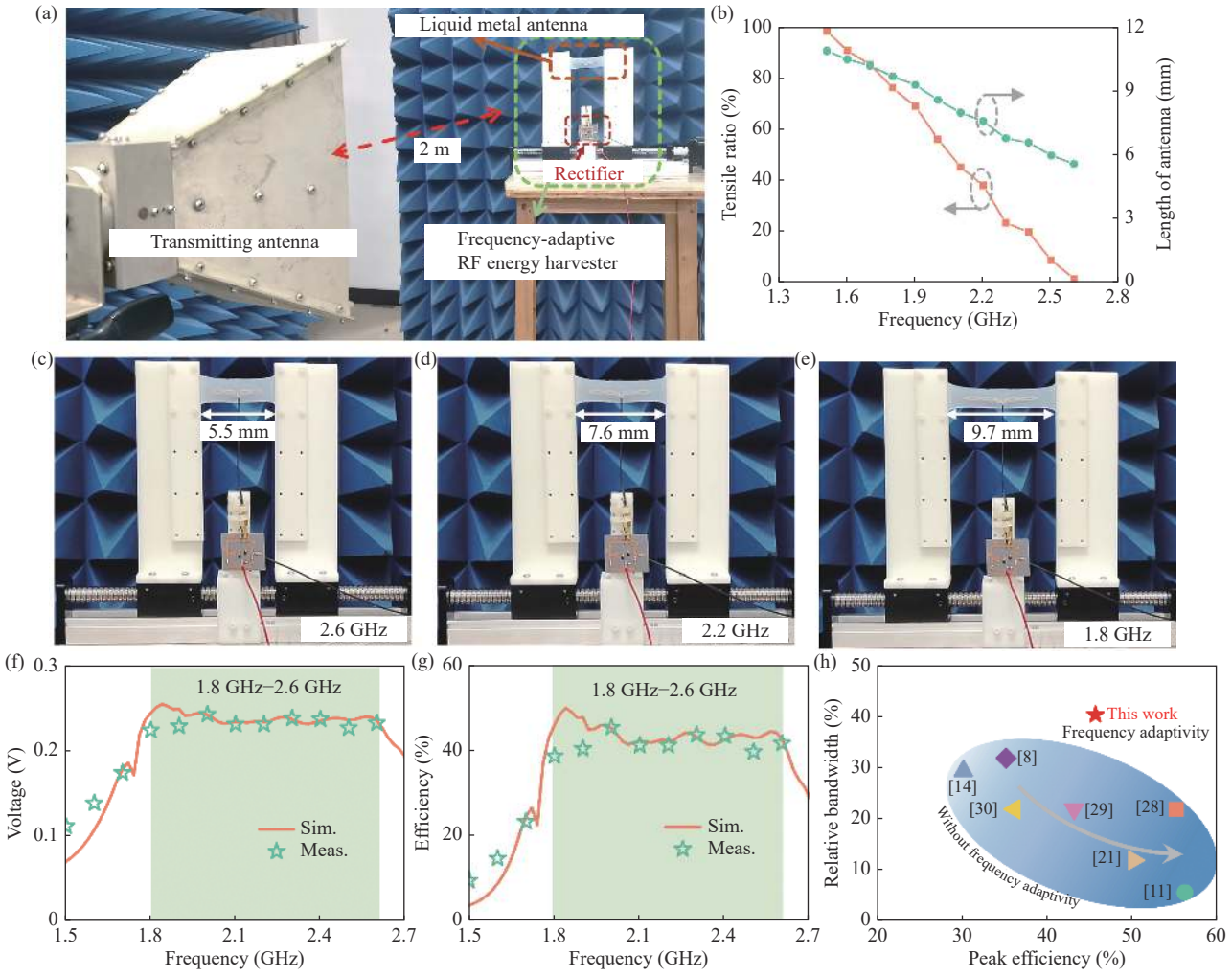

Figure 8 (a) Measurement photograph for the proposed frequency-self-adaptive RF energy harvester. (b) Measured tensile ratio and length of the antenna as a function of operation frequency. (c)–(e) Measured stretched state and length of the LM-based antenna corresponding to each frequency. Measured and simulated (f) Output DC voltage and (g) RF-DC efficiency of the proposed RF energy harvester as a function of frequency. (h) A comparison between our design with related designs.

carefully selecting components, the power consumption of the step motor can be reduced to as low as 0.05 W, while the MCU can operate on as little as 47.14 μW. This significantly lowers the power demands, making the system suitable for low-power IoT infrastructures. Moreover, the potential applications of our design extend beyond frequency-adaptive RF energy harvesting; it could also be used for wireless ambient frequency and power sensing in future applications.

Finally, a comparison between our rectenna design and some recent rectenna and rectifier designs is given in Table 2. Comprehensively considering the radiation pattern stability, RF-DC conversion efficiency, and relative bandwidth, our design exhibits significant superiority over all others listed in Table 2. Although the peak RF-DC efficiency of the proposed rectenna is slightly lower than those reported in [11], [21], [28], our design still successfully breaks the traditional trade-off between peak efficiency and relative bandwidth, as demonstrated in Figure 8(h). In addition, our design appears to be the only one with frequency adaptivity, making it an excellent candidate for RF energy harvesting in numerous practical applications.

IV. Conclusion

In this study, we have introduced a pioneering solution for RF energy harvesting – mechanical frequency-self-adaptive RF power harvester empowered by a dual "∞"-shaped antenna and reconfigurable LM. This innovation allows for continuous tuning of the system's working frequency within the range of 1.8 to 2.6 GHz by applying external mechanical strain to the LM antenna. The integration of a tailored control logic into MCU enables automatic frequency adjustment and identification when exposed to specific signals. Simultaneously, the proposed system exhibits impressive rectification efficiency, yielding a rapid generation of DC power exceeding 0.25 V at an input power level of −10 dBm. This harvested DC power is readily accessible for direct utilization. Experimental validation serves as a testament to the system's adaptability and robust performance across diverse operational conditions. These results

Table 2 Comparison of our design with other related works

Ref.	Radiation direction of antenna at all working bands	Radiation pattern stability	PCE at –10 dBm (%)	Operation band (GHz) (≥ 80% × PCE)	Relative bandwidth (%)	Technique	Frequency adaptivity
[8]	NR	NR	35	0.84–1.16	32	Series	No
[11]	Non-omnidirectional	NR	56	2.38–2.52	5.7	Series	No
[14]	NR	NR	30	1.1–1.48	29.5	Double voltage	No
[21]	NR	NR	50	0.86–0.97	12	Conjugate matching	No
[28]	Non-omnidirectional	No	55	1.79–2.27	23.6	Double voltage	No
[29]	NR	NR	43	0.73–0.92	23	Double voltage	No
[30]	NR	NR	36	1.11–1.39	22.4	Double voltage	No
This work	Omnidirectional	Yes	45.5	1.75–2.65	40.9	Shunt	Yes

Note: NR, not reported; PCE, peak conversion efficiency.

hold significant promise in effectively harnessing RF energy from spatiotemporal-varying environments. In summary, our work presents a dynamic and self-adapting approach to RF energy harvesting. The synergy between frequency tuning and efficient rectification addresses the challenge of effectively capturing RF energy within an ever-changing spectrum. The successful experimental validation attests to the system's efficacy, showcasing its potential to address the intricate demands of RF energy harvesting in dynamic environments. This innovation marks a significant stride towards sustainable energy solutions. These results hold significant promise in effectively harnessing RF energy from spatiotemporal-varying environments. In summary, our work presents a dynamic and self-adapting approach to RF energy harvesting. The synergy between frequency tuning and efficient rectification addresses the challenge of effectively capturing RF energy within an ever-changing spectrum. The successful experimental validation attests to the system's efficacy, showcasing its potential to address the intricate demands of RF energy harvesting in dynamic environments. This innovation marks a significant stride towards sustainable energy solutions.

Acknowledgements

This work was supported in part by the National Natural Science Foundation of China (Grant No. 62101394), the National Science Fund for Distinguished Young Scholars (Grant No. 62225108), the Foundation from the Guangxi Key Laboratory of Optoelectronic Information Processing (Grant No. GD21203), and the Beijing Nova Program (Grant No. 2304842874).

Supporting Information

Supplementary Note S1, Fig. S1, Tables S1 to S2 and Video S1. The supporting information is available online at www.emscience.org. The supporting materials are published as submitted, without typesetting or editing. The responsibility for scientific accuracy and content remains entirely with the authors.

References

[1] R. Sharma, R. Mishra, T. Ngo, *et al*., "Electrically connected spin-torque oscillators array for 2.4 GHz WiFi band transmission and energy harvesting," *Nature Communications*, vol. 12, no. 1, article no. 2924, 2021.

[2] J. M. Li, Y. L. Dong, J. H. Park, *et al*., "Body-coupled power transmission and energy harvesting," *Nature Electronics*, vol. 4, no. 7, pp. 530–538, 2021.

[3] M. De Cea, A. H. Atabaki, and R. J. Ram, "Energy harvesting optical modulators with sub-attojoule per bit electrical energy consumption," *Nature Communications*, vol. 12, no. 1, article no. 2326, 2021.

[4] C. Xu and Z. L. Wang, "Compact hybrid cell based on a convoluted nanowire structure for harvesting solar and mechanical energy," *Advanced Materials*, vol. 23, no. 7, pp. 873–877, 2011.

[5] Q. Zhang, Q. J. Liang, D. K. Nandakumar, *et al*., "Shadow enhanced self-charging power system for wave and solar energy harvesting from the ocean," *Nature Communications*, vol. 12, no. 1, article no. 616, 2021.

[6] J. R. Tritsch, W. L. Chan, X. Wu, *et al*., "Harvesting singlet fission for solar energy conversion via triplet energy transfer," *Nature Communications*, vol. 4, no. 1, article no. 2679, 2013.

[7] Y. N. Ouyang, W. Zhao, and H. F. Wang, "Simulation and study of maximum power point tracking for rim-driven tidal current energy power generation systems," *Energy Reports*, vol. 9, pp. 792–801, 2023.

[8] G. Le, N. Nguyen, N. D. Au, *et al*., "A broadband high-efficiency rectifier for mid-field wireless power transfer," *IEEE Microwave and Wireless Components Letters*, vol. 31, no. 7, pp. 913–916, 2021.

[9] K. W. Pan, Y. Y. Fan, T. Leng, *et al*., "Sustainable production of highly conductive multilayer graphene ink for wireless connectivity and IoT applications," *Nature Communications*, vol. 9, no. 1, article no. 5197, 2018.

[10] X. Zhang, J. Grajal, J. L. Vazquez-Roy, *et al*., "Two-dimensional MoS_2-enabled flexible rectenna for Wi-Fi-band wireless energy harvesting," *Nature*, vol. 566, no. 7744, pp. 368–372, 2019.

[11] S. E. Adami, P. Proynov, G. S. Hilton, *et al*., "A flexible 2.45-GHz power harvesting wristband with net system output from –24.3 dBm of RF power," *IEEE Transactions on Microwave Theory and Techniques*, vol. 66, no. 1, pp. 380–395, 2018.

[12] L. M. Jiang, Y. Yang, R. M. Chen, *et al*., "Flexible piezoelectric ultrasonic energy harvester array for bio-implantable wireless generator," *Nano Energy*, vol. 56, pp. 216–224, 2019.

[13] J. Zhu, Z. H. Hu, C. Y. Song, *et al*., "Stretchable wideband dipole antennas and rectennas for RF energy harvesting," *Materials Today Physics*, vol. 18, article no. 100377, 2021.

[14] W. B. Liu, K. M. Huang, T. Wang, *et al*., "A broadband high-efficiency RF rectifier for ambient RF energy harvesting," *IEEE Microwave and Wireless Components Letters*, vol. 30, no. 12, pp. 1185–1188, 2020.

[15] Z. C. Chen, Q. H. Li, L. J. Wu, *et al*., "Optimal data collection of

multi-radio multi-channel multi-power wireless sensor networks for structural monitoring applications: A simulation study," *Structural Control and Health Monitoring*, vol. 26, no. 4, article no. e2328, 2019.

[16] K. Skarżyński and M. Słoma, "Printed electronics in radiofrequency energy harvesters and wireless power transfer rectennas for IoT applications," *Advanced Electronic Materials*, vol. 9, no. 8, article no. 2300238, 2023.

[17] W. W. Li, H. R. Zhang, S. Kagita, *et al*., "All screen-printed, polymer-nanowire based foldable electronics for mm-wave applications," *Advanced Materials Technologies*, vol. 6, no. 11, article no. 2100525, 2021.

[18] Y. Z. Wang, T. C. Guo, Z. N. Tian, *et al*., "MXenes for energy harvesting," *Advanced Materials*, vol. 34, no. 21, article no. 2108560, 2022.

[19] D. H. Kim, H. J. Shin, H. Lee, *et al*., "In vivo self-powered wireless transmission using biocompatible flexible energy harvesters," *Advanced Functional Materials*, vol. 27, no. 25, article no. 1700341, 2017.

[20] I. Tavakkolnia, L. K. Jagadamma, R. Bian, *et al*., "Organic photovoltaics for simultaneous energy harvesting and high-speed MIMO optical wireless communications," *Light: Science & Applications*, vol. 10, no. 1, article no. 41, 2021.

[21] J. Tissier and M. Latrach, "A 900/1800 MHz dual-band high-efficiency rectenna," *Microwave and Optical Technology Letters*, vol. 61, no. 5, pp. 1278–1283, 2019.

[22] B. N. Wang, K. H. Teo, T. Nishino, *et al*., "Experiments on wireless power transfer with metamaterials," *Applied Physics Letters*, vol. 98, no. 25, article no. 254101, 2011.

[23] H. T. Zhao, Y. Shuang, M. L. Wei, *et al*., "Metasurface-assisted massive backscatter wireless communication with commodity Wi-Fi signals," *Nature Communications*, vol. 11, no. 1, article no. 3926, 2020.

[24] S. Shang, S. Z. Yang, J. Liu, *et al*., "Metamaterial electromagnetic energy harvester with high selective harvesting for left- and right-handed circularly polarized waves," *Journal of Applied Physics*, vol. 120, no. 4, article no. 045106, 2016.

[25] M. Zaeimbashi, M. Nasrollahpour, A. Khalifa, *et al*., "Ultra-compact dual-band smart NEMS magnetoelectric antennas for simultaneous wireless energy harvesting and magnetic field sensing," *Nature Communications*, vol. 12, no. 1, article no. 3141, 2021.

[26] Y. X. Zhang, C. F. Pan, P. F. Liu, *et al*., "Coaxially printed magnetic mechanical electrical hybrid structures with actuation and sensing functionalities," *Nature Communications*, vol. 14, no. 1, article no. 4428, 2023.

[27] J. Ausra, S. J. Munger, A. Azami, *et al*., "Wireless battery free fully implantable multimodal recording and neuromodulation tools for songbirds," *Nature Communications*, vol. 12, no. 1, article no. 1968, 2021.

[28] C. Y. Song, Y. Huang, J. F. Zhou, *et al*., "A high-efficiency broadband rectenna for ambient wireless energy harvesting," *IEEE Transactions on Antennas and Propagation*, vol. 63, no. 8, pp. 3486–3495, 2015.

[29] H. S. Park and S. K. Hong, "Broadband RF-to-DC rectifier with uncomplicated matching network," *IEEE Microwave and Wireless Components Letters*, vol. 30, no. 1, pp. 43–46, 2020.

[30] W. B. Liu, K. M. Huang, T. Wang, *et al*., "Broadband high-efficiency RF rectifier with a cross-shaped match stub of two one-eighth-wavelength transmission lines," *IEEE Microwave and Wireless Components Letters*, vol. 31, no. 10, pp. 1170–1173, 2021.

[31] J. Kimionis, A. Collado, M. M. Tentzeris, *et al*., "Octave and decade printed UWB rectifiers based on nonuniform transmission lines for energy harvesting," *IEEE Transactions on Microwave Theory and Techniques*, vol. 65, no. 11, pp. 4326–4334, 2017.

[32] M. Cansiz, D. Altinel, and G. K. Kurt, "Efficiency in RF energy harvesting systems: A comprehensive review," *Energy*, vol. 174, pp. 292–309, 2019.

[33] L. Li, X. M. Zhang, C. Y. Song, *et al*., "Progress, challenges, and perspective on metasurfaces for ambient radio frequency energy harvesting," *Applied Physics Letters*, vol. 116, no. 6, article no. 060501, 2020.

[34] Z. H. Nie, H. Q. Zhai, L. H. Liu, *et al*., "A dual-polarized frequency-reconfigurable low-profile antenna with harmonic suppression for 5G application," *IEEE Antennas and Wireless Propagation Letters*, vol. 18, no. 6, pp. 1228–1232, 2019.

[35] A. Boukarkar, X. Q. Lin, Y. Jiang, *et al*., "A compact frequency-reconfigurable 36-states patch antenna for wireless applications," *IEEE Antennas and Wireless Propagation Letters*, vol. 17, no. 7, pp. 1349–1353, 2018.

[36] S. C. Chiu, L. Y. O. Yang, C. P. Lai, *et al*., "Compact CRLH asymmetric-CPS resonant antenna with frequency agility," *IEEE Transactions on Antennas and Propagation*, vol. 62, no. 2, pp. 527–534, 2014.

[37] M. S. Alam and A. Abbosh, "A compact reconfigurable antenna with wide tunable frequency and 360° beam scanning," *IEEE Antennas and Wireless Propagation Letters*, vol. 18, no. 1, pp. 4–8, 2019.

[38] S. H. Zhang, J. Zhu, Y. Y. Zhang, *et al*., "Standalone stretchable RF systems based on asymmetric 3D microstrip antennas with on-body wireless communication and energy harvesting," *Nano Energy*, vol. 96, article no. 107069, 2022.

[39] Z. C. Song, J. F. Zhu, X. C. Wang, *et al*., "Origami metamaterials for ultra-wideband and large-depth reflection modulation," *Nature Communications*, vol. 15, no. 1, article no. 3181, 2024.

[40] S. Liu, S. J. Ma, R. W. Shao, *et al*, "Moiré metasurfaces for dynamic beamforming," *Science Advances*, vol. 8, no. 33, article no. eabo1511, 2022.

[41] S. I. H. Shah and S. Lim, "RF advancements enabled by smart shape memory materials in the microwave regime: A state-of-the-art review," *Materials Today Physics*, vol. 44, article no. 101435, 2024.

[42] J. Ma, F. Krisnadi, M. H. Vong, *et al*., "Shaping a soft future: Patterning liquid metals," *Advanced Materials*, vol. 35, no. 19, article no. 2205196, 2023.

[43] Z. D. He, Y. W. Wang, H. Y. Xiao, *et al*., "Highly stretchable, deformation-stable wireless powering antenna for wearable electronics," *Nano Energy*, vol. 112, article no. 108461, 2023.

[44] Y. C. Wang, Y. T. Lu, D. Q. Mei, *et al*., "Liquid metal-based wearable tactile sensor for both temperature and contact force sensing," *IEEE Sensors Journal*, vol. 21, no. 2, pp. 1694–1703, 2021.

[45] F. Lazzari, M. Gaviati, L. Garavaglia, *et al*., "A liquid-metal wearable sensor for respiration monitoring: Biomechanical requirements, modeling, design, and characterization," *IEEE Sensors Journal*, vol. 23, no. 6, pp. 6243–6253, 2023.

[46] H. L. He, Y. Wu, Z. Yang, *et al*., "Study of liquid metal fault current limiter for medium-voltage DC power systems," *IEEE Transactions on Components, Packaging and Manufacturing Technology*, vol. 8, no. 8, pp. 1391–1400, 2018.

[47] S. Alkaraki, Q. W. Lin, J. R. Kelly, *et al*., "Phased array antenna system enabled by liquid metal phase shifters," *IEEE Access*, vol. 11, pp. 96987–97000, 2023.

[48] A. Dey and G. Mumcu, "Microfluidically controlled frequency-tunable monopole antenna for high-power applications," *IEEE Antennas and Wireless Propagation Letters*, vol. 15, pp. 226–229, 2016.

[49] A. P. Saghati, J. S. Batra, J. Kameoka, *et al*., "A microfluidically reconfigurable dual-band slot antenna with a frequency coverage ratio of 3 : 1," *IEEE Antennas and Wireless Propagation Letters*, vol. 15, pp. 122–125, 2016.

[50] A. M. Morishita, C. K. Y. Kitamura, A. T. Ohta, *et al*., "A liquid-metal monopole array with tunable frequency, gain, and beam steering," *IEEE Antennas and Wireless Propagation Letters*, vol. 12, pp. 1388–1391, 2013.

[51] A. Arbelaez, I. Goode, J. Gomez-Cruz, *et al*., "Liquid metal reconfigurable patch antenna for linear, RH, and LH circular polarization with frequency tuning," *Canadian Journal of Electrical and Com-*

puter Engineering, vol. 43, no. 4, pp. 218–223, 2020.
[52] T. T. Zhang, Y. K. Chen, and S. W. Yang, "A wideband frequency- and polarization-reconfigurable liquid metal-based spiral antenna," *IEEE Antennas and Wireless Propagation Letters*, vol. 21, no. 7, pp. 1477–1481, 2022.
[53] L. N. Song, W. R. Gao, C. O. Chui, *et al*., "Wideband frequency reconfigurable patch antenna with switchable slots based on liquid metal and 3-D printed microfluidics," *IEEE Transactions on Antennas and Propagation*, vol. 67, no. 5, pp. 2886–2895, 2019.
[54] J. Zhu, J. J. Fox, N. Yi, *et al*., "Structural design for stretchable microstrip antennas," *ACS Applied Materials & Interfaces*, vol. 11, no. 9, pp. 8867–8877, 2019.
[55] Z. Li, T. R. Le, Z. K. Wu, *et al*., "Rational design of a printable, highly conductive silicone-based electrically conductive adhesive for stretchable radio-frequency antennas," *Advanced Functional Materials*, vol. 25, no. 3, pp. 464–470, 2015.
[56] M. Kubo, X. F. Li, C. Kim, *et al*., "Stretchable microfluidic radiofrequency antennas," *Advanced Materials*, vol. 22, no. 25, pp. 2749–2752, 2010.
[57] T. Chang, Y. Tanabe, C. C. Wojcik, *et al*., "A general strategy for stretchable microwave antenna systems using serpentine mesh layouts," *Advanced Functional Materials*, vol. 27, no. 46, article no. 1703059, 2017.
[58] X. Geng, M. Su, Y. M. Zhang, *et al*., "Pattern-reconfigurable liquid metal magneto-electric dipole antenna," *IEEE Antennas and Wireless Propagation Letters*, vol. 21, no. 8, pp. 1683–1687, 2022.
[59] X. Bai, M. Su, Y. A. Liu, *et al*., "Wideband pattern-reconfigurable cone antenna employing liquid-metal reflectors," *IEEE Antennas and Wireless Propagation Letters*, vol. 17, no. 5, pp. 916–919, 2018.
[60] K. Y. Alqurashi, J. R. Kelly, Z. P. Wang, *et al*., "Liquid metal bandwidth-reconfigurable antenna," *IEEE Antennas and Wireless Propagation Letters*, vol. 19, no. 1, pp. 218–222, 2020.
[61] W. Chen, Y. D. Li, R. Li, *et al*., "Bendable and stretchable microfluidic liquid metal-based filter," *IEEE Microwave and Wireless Components Letters*, vol. 28, no. 3, pp. 203–205, 2018.
[62] X. Q. Lin, P. Mei, P. C. Zhang, *et al*., "Development of a resistor-loaded ultrawideband absorber with antenna reciprocity," *IEEE Transactions on Antennas and Propagation*, vol. 64, no. 11, pp. 4910–4913, 2016.
[63] Y. Luo and Z. N. Chen, "Compressed dipoles resonating at higher order modes with enhanced directivity," *IEEE Transactions on Antennas and Propagation*, vol. 65, no. 11, pp. 5697–5701, 2017.

Cheng Zhang was born in Henan Province, China. He received the M.S. degree in material science and technology from Wuhan University of Technology, Wuhan, China, in 2015, and the Ph.D degree at the State Key Laboratory of Millimeter Waves, Department of Radio Engineering, Southeast University, Nanjing, in 2019. He is currently a Professor in Shanghai Institute of Optics and Fine Mechanics, Chinese Academy of Sciences, Shanghai, China. His current research interests are EM energy harvesting, stealth metamaterial/metasurface and multi-physical manipulation. He has authored or co-authored more than fifty publications (including six highly cited papers), with citation over 2000 times. Dr. Zhang was a recipient of the 2020 CHINA TOP CITED PAPER AWARD from IOP Publishing and Top Articles in Device Physics for Applied Physics Letters (two papers). He received the Honor mention award for best student paper contest in 2018 IEEE International Workshop on Antenna Technology (iWAT) and the Appreciation award of invited talk in 2018 IEEE International Conference on Computational Electromagnetics (ICCEM).
(Email: czhangseu@foxmail.com)

Yuchao Wang received the B.S. degree in electronic science and technology from the Wuhan University of Technology, Wuhan, China, in 2018, where he received the M.S. degree in 2021. He is currently pursuing the Ph.D. degree at Wuhan University of Technology, Wuhan, China. He has been a joint Ph.D. Student Scholar at Shanghai Institute of Optics and Fine Mechanics, Chinese Academy of Sciences, Shanghai, China, since 2024. His research interests include planar antennas, RF energy harvesting, and wireless power transmission.
(Email: yuchao9629@whut.edu.cn)

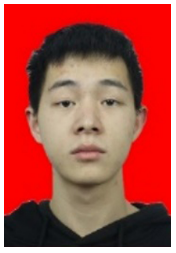

Zebin Zhu received the B.S. degree from the Wuhan University of Technology, Wuhan, China, in 2021, where he is pursuing the M.S. degree. He has been a joint M.S. Student Scholar at Shanghai Institute of Optics and Fine Mechanics, Chinese Academy of Sciences, Shanghai, China, since 2024. His research interests include antenna array, and wireless power transmission.
(Email: ze1704@whut.edu.cn)

Hai Lin was born in Hubei Province, China, in 1978. He received the B.E. degree in electrical engineering from Wuhan University, Wuhan, China, in 2000, and the M.S. degree in microwave technology and the Ph.D. degree in computer science from Wuhan University, Wuhan China, in 2002 and 2006, respectively. In 2006, he joined as a Lecturer the College of Physical Science and Technology, Central China Normal University, Wuhan, China, where he became an Associate Professor in 2009. From December 2011 to September 2012, he was with the Department of Electromagnetics and Solid Physics, University of Granada, Granada, Spain, where he was also a Postdoctoral Researcher. From December 2013 to December 2014, he was a Marie-Curie Experience Researcher with the Department of Electrical Engineering, Queen Mary University of London, UK. He is a Member of IEEE. His current research interests include computational electromagnetics, 5G communication, base station antenna, and metasurface antenna.
(Email: linhai@mail.ccnu.edu.cn)

Kun Wang was born in Sichuan Province, China, in 2000. He received the B.E degree from China West Normal University, Nanchong, China, in 2022. He is currently pursuing the M.S. degree in Central China Normal University, Wuhan, China. His current research interests include reconfigurable intelligent surfaces, wireless power transfer, and energy harvesting.
(Email: wkphy@mails.ccnu.edu.cn)

Xintong Shi was born in Hebei Province, China, in 1993. He received the B.E. degree in communication engineering from the Mingde College, Northwestern Polytechnical University, Xi'an, China, in 2017, and the M.S. degree in instrumentation engineering form the Guilin University of Electronic Technology, Guilin, China, in 2020. He is currently pursuing the Ph.D. degree in Central China Normal University, Wuhan, China. His current research interests include terahertz multi-function devices and metamaterials research.

(Email: shxt@mails.ccnu.edu.cn)

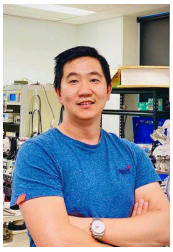

Yi Du received the B.E. degree from the School of Materials Science and Engineering, Beihang University, Beijing China, in 2004 and the Ph.D. degree from the Institute for Superconducting and Electronic Materials at University of Wollongong, Wollongong, New South Wales, Australia, in 2011. He is currently a Professor with the School of Physics, Beihang University, Beijing, China. His research interests include exploration of low-dimensional quantum matters, studies of novel surface physical and chemical properties in two-dimensional materials, and studies of renewable energy conversion processes by using scanning tunneling microscopy and angle-resolved photoemission spectroscopy.
(Email: yi_du@buaa.edu.cn)

Chaoyun Song received the B.E. M.S., and Ph.D. degrees in electrical engineering and electronics from University of Liverpool, Liverpool, UK, in 2012, 2013, and 2017, respectively. He is currently an Associate Professor (Senior Lecturer) with the Department of Engineering, King's College London, London, UK. He is also a Professor with State Key Laboratory of Radio Frequency Heterogeneous Integration, College of Electronics and Information Engineering, Shenzhen University, Shenzhen, China. Prior to this, he was an Assistant Professor with the School of Engineering and Physical Sciences, Heriot-Watt University, Edinburgh, Scotland, UK. He has published more than 110 papers (including 45 IEEE transactions) in peer-reviewed journals and conference proceedings. He is a Senior Member of IEEE. His current research interests include wireless energy harvesting and power transfer, rectifying antennas (rectennas), flexible and stretchable electronics, metamaterials and meta-surface, and low-power sensors. Dr. Song has been the recipient of numerous international awards, including the IEEE AP-S Young Professional Ambassador 2023, IEEE AP-S Raj Mittra Travel Grant 2023, EuCAP 2023 Best Antenna Paper Award, IET Innovation Award in 2018, and BAE Systems Chairman's Award in 2017. Additionally, Dr. Song has served as a Session Chair and/or TPC Member for various conferences, including EuCAP2018, IEEE AP-S Symposium 2021, IEEE VTC2022-fall, EuCAP2023, IEEE AP-S Symposium 2023 and EuCAP2024. He has consistently contributed as a reviewer for esteemed journals such as *Nature Electronics*, *Nature Communications*, *Advanced Materials*, *Advanced Functional Materials*, and *Nano Energy*, in addition to reviewing for over fifteen IEEE Transactions. He is a Top-200 reviewer for *IEEE Transactions on Antenna and Propagation* (2021–2023). He has also taken on the role of Guest Editor for prestigious publications including *IEEE Open Journal on Antennas and Propagation*, *IET Electronic Letters*, *Micromachines*, and *Wireless Communications and Mobile Computing* and an Associate Editor for *Frontiers in Communications and Networks*.
(Email: chaoyun.song@kcl.ac.uk)

Long Ren received the Ph.D. degree in materials science from the University of Wollongong, Wollongong, New South Wales, Australia, in 2019. He is currently a Professor with the International School of Materials Science and Engineering, Wuhan University of Technology, Wuhan, China. His current research focuses on the design and synthesis of liquid metal and the relevant hybrids as smart functional materials, for micro/nanorobots and energy devices.
(Email: renlong@whut.edu.cn)

Qiang Cheng received the B.S. and M.S. degrees from Nanjing University of Aeronautics and Astronautics, Nanjing, China, in 2001 and 2004, respectively, and the Ph.D. degree from Southeast University, Nanjing, China, in 2008. In 2008, he joined the State Key Laboratory of Millimeter Waves, Southeast University, Nanjing, China, where he was involved in the development of metamaterials and metadevices. He is currently a Full Professor with the Radio Department, Southeast University, Nanjing, China. He leads a group of Ph.D. students and master students in the area of metamaterials, tunable microwaves circuits, microwave imaging, and terahertz systems. He has authored or co-authored more than one hundred publications, with citation over 2000 times. Dr. Cheng was a recipient of the 2010 Best Paper Award from the *New Journal of Physics*, the Chinas Top Ten Scientific Advances of 2010, and the Second Class National Natural Science Award in 2014. He served as the Vice Chair for the 2008 and 2010 International Workshop on Metamaterials, Nanjing, China.
(Email: qiangcheng@seu.edu.cn)